JOURNAL OF MATERIALS SCIENCE 35 (2000) 655–660

The Crystalline quality of $In_xAl_{1-x}As$ layers on InP grown by molecular beam epitaxy at 520°C

J. S. CHOI, T. S. OH, W. K. CHOO
Department of Materials Science and Engineering, Korea Advanced Institute of Science and Technology, Tae-Jeon, Korea

The crystalline quality of $In_xAl_{1-x}As$ ($x = 0.52$, 0.489, 0.476) layers grown by molecular beam epitaxy (MBE) on InP substrate at 520°C has been studied. From the double crystal x-ray diffraction and photoluminescence measurement, $In_xAl_{1-x}As$ ($x = 0.52$, 0.489) layers have been found to reveal high quality crystallinity and excellent optical performance. Although the $In_{0.489}Al_{0.511}As$ layer of thickness of 1.116 μm has a lattice mismatch of 0.23%, an excellent lattice coherency has been achieved. On the other hand, in the $In_{0.476}Al_{0.524}As$ layer which has only a slightly larger lattice mismatch of 0.32%, stacking faults are observed. We have also observed the modulation contrast in planar view images obtained from transmission electron microscopy, which most likely arises due to the clustering of In or Al atoms. The modulation has a wavelength of about 8 nm independent of the lattice mismatch between the substrate and the epilayer.

1. Introduction

$In_xAl_{1-x}As$/InP heterostructure is of great technological interest for microwave, optoelectronic, and fast electronic device applications. An important aspect for improved performance of the heterostructure devices is to fabricate the ultra-thin layers of high quality heterostructure with atomistically smooth interface. So far, this material has been grown mainly by molecular beam epitaxy (MBE). Due to the high Al content, however, the crystalline and optical properties of the epilayers are found to be rather poorer than the other pseudobinary III-V compound semiconductor alloys such as InGaAs [1–3]. To avoid In desorption which occurs at temperatures higher than 500–530°C [4–6], it is necessary to grow InAlAs layers at low temperatures. Moreover, the InAlAs system shows significant clustering due to the large difference between In–As and Al–As bond energies at low temperatures employed in MBE growth [7–10]. It was known that clustering generally has a detrimental effect on the optical and transport properties of materials [11, 12].

In regards to clustering that occurs in MBE-grown InAlAs layers, Sigh *et al.* [8] have demonstrated the dependence of clustering on growth temperature by the Monte Carlo simulation. From the optical and transport properties of InAlAs layer grown by MBE in the temperature range of 300–520°C, it was reported that clustering effect becomes most severe at intermediate temperatures [13]. Some other investigators [14, 15] have suggested that the InAlAs layer of both high structural perfection and excellent optical performance could be grown at high substrate temperatures because the atomic clustering can be suppressed. So far, the clustering in InAlAs layers has been studied exclusively by investigation of the optical and transport properties. However, a combination of TEM and x-ray diffraction investigations on clustering in InAlAs layers in association with photoluminescence have not been conducted up to our knowledge, although it is very important to control clustering and thus to achieve the high crystal quality of InAlAs layer.

In this work, we have studied the crystalline quality of differently lattice mismatched InAlAs/InP layers grown by MBE by double-crystal x-ray diffraction (DCXD), photoluminescence (PL), conventional and high resolution transmission electron microscopy. From the thorough transmission electron microscopy investigation, we also conducted the direct observation of the clustering in epilayers. The relaxation of the InAlAs layer having a rather large lattice mismatch has also been examined.

2. Experimental procedure

The $In_xAl_{1-x}As$ layers ($x = 0.52$, 0.489, 0.476) were grown on Fe-doped semi-insulating (001) InP substrates in a Riber MBE 45 system at 520°C. To desorb the native oxide the growth, the InP substrates were heated up to 450°C and kept for 20 min under a typical As_4 flux. In order to prevent the formation of As-induced defects, if possible, the As cell temperature had been adjusted to give a total pressure of about 1.5×10^{-7} torr during layer growth. Also, the V/III beam equivalent pressure was kept 10. The growth rate was kept at 1 μm/hr.

The structural properties of the specimens were investigated on a computer-controlled Rigaku Bede type

DCXD. The optical properties were assessed by PL. The PL measurements were performed at 77 K using an Ar^+ laser emitting at 514.5 nm. The luminescence was recorded by using a cool Ge detector and a standard lock-in amplifier.

All the specimens for transmission electron microscopy were prepared by mechanical polishing to a thickness of 20 μm and subsequent ion-beam milling with Ar^+ at low voltage and intensities in a liquid nitrogen cooled stage by Gatan Duo-Mill 600 DIF to avoid the formation of In island. Especially the specimens for planar view were ion-milled at the substrate side. Our conventional TEM observations were carried out at 200 kV using Philips CM20 and Jeol JEM 2000FX microscope, whereas the high resolution TEM studies were conducted with a Joel JEM 2000EX equipped a top-entry specimen holder.

3. Results and discussion

3.1. The crystalline quality of $In_{0.52}Al_{0.48}As$ and $In_{0.489}Al_{0.511}As$ layers

The theoretical full width at half maximum (FWHM) of the (004 line for InAlAs layer, by simulations using dynamic theory based on perfect crystal, is known as a function of layer thickness [16]. The theoretical values of FWHM for $In_{0.52}Al_{0.48}As$ ($t = 1.156$ μm) and $In_{0.489}Al_{0.476}As$ ($t = 1.116$ μm) layers are calculated to be 19 and 18 arcsecond, respectively. The lattice parameter of $In_{0.52}Al_{0.48}As$ artificially matches that of InP. The meawured FWHM value of the latter is same as the theoretical one. This result indicates that InAlAs layers with a very high crystalline quality have been grown at the aforementioned growth condition in spite of the lattice misfit of 0.23%.

Fig. 1a and b show the (004) rocking curves recorded respectively from $In_{0.52}Al_{0.48}As$ and $In_{0.489}Al_{0.511}As$ layers. The FWHM of a double crystal x-ray diffraction peak is often cited as a merit figure of the crystalline quality of epitaxial layers since it is sensitive to crystalline imperfections. The FWHM of the $In_{0.489}Al_{0.511}As$ layer peak was measured to be 18 arcsecond. This value is so far the smallest reported one for the FWHM of InAlAs layers grown directly on InP substrates. In the case of $In_{0.52}Al_{0.48}As$ layer, we could not separately measure the FWHM of the layer line due to the closeness of two lines from the substrate. However, it is obvious that its FWHM is smaller than 35 arcsecond. The FWHM of the epilayer of the former alloy is not fully resolved from that of the InP substrate (Fig. 1a). The overall width, 35 arcsecond, is roughly twice that of the individual FWHM both of the substrate and the epilayer which are respectively about 18 arcsecond.

The TEM microstructure, obtained from $In_{0.52}Al_{0.48}As$ and $In_{0.489}Al_{0.511}As$ layers, are shown in Figs 2 and 3 respectively. No extended defects such as dislocations and stacking fault deteriorating the crystalline quality of epitaxial layers are observed in our specimens. These two figures support the X-ray diffraction evidences.

Clustering in the InAlAs layers on InP was known to render an adverse effect on the quality of epilayers

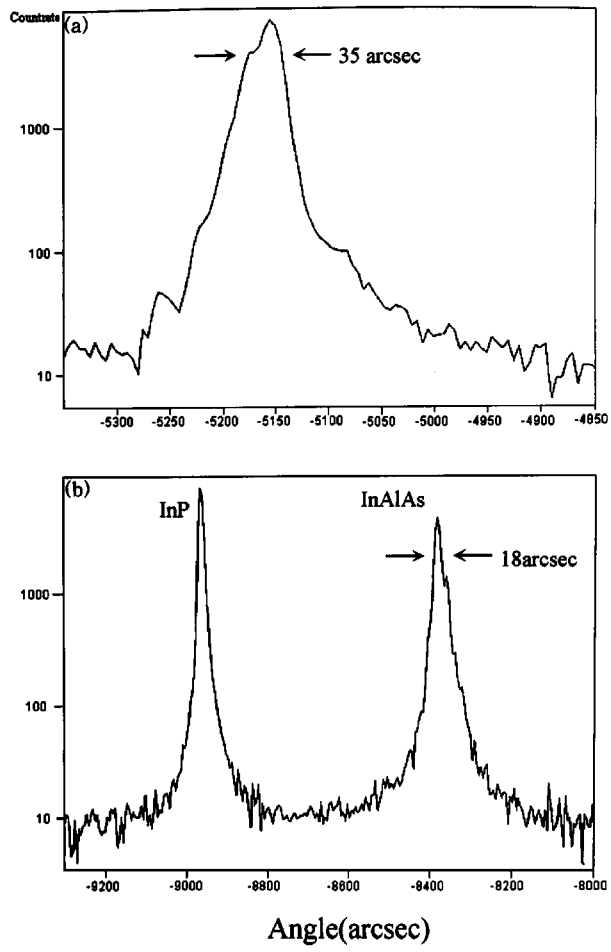

Figure 1 Double crystal x-ray diffraction patterns in vicinity of the (004) InP reciprocal lattice of the $In_xAl_{1-x}As$ layers; (a) $In_{0.52}Al_{0.48}As$ and (b) $In_{0.489}Al_{0.511}As$. Notice that the intensity is displayed on the logarismic scale.

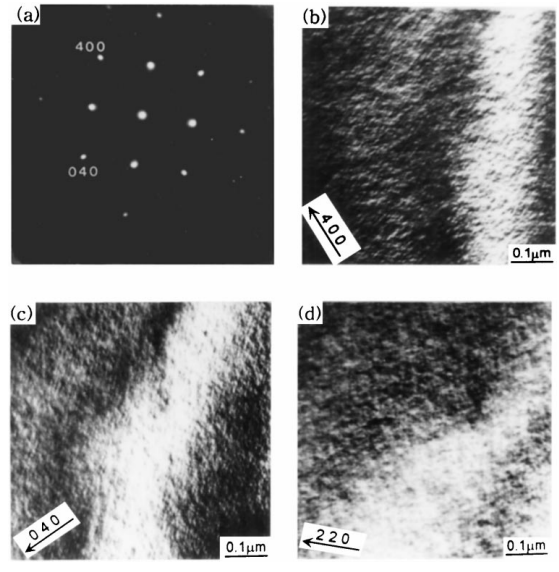

Figure 2 TEM planar view of $In_{0.52}Al_{0.48}As$ layer; (a) diffraction pattern in [001] zone, and (b), (c) and (d) are a series of DF images taken in 400, 040 and 220 reflections, respectively.

[11, 12, 14, 15]. For InGaAs as for InAlAs, several investigations have already been performed on the microstructure change initiated by clustering that occurs during growth [17–19]. The clustering causes modulation contrasts aligned along the [100] and [010] directions in TEM two-beam images and their size is known

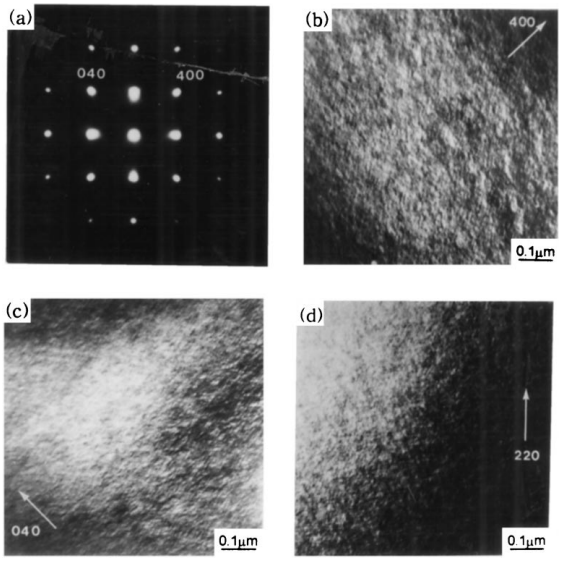

Figure 3 TEM planar view of $In_{0.489}Al_{0.511}As$ layer (a) [001] zone diffraction pattern. (b), (c) and (d) are series of DF image obtained from specimen in (400), (040) and (220) two beam conditions, respectively.

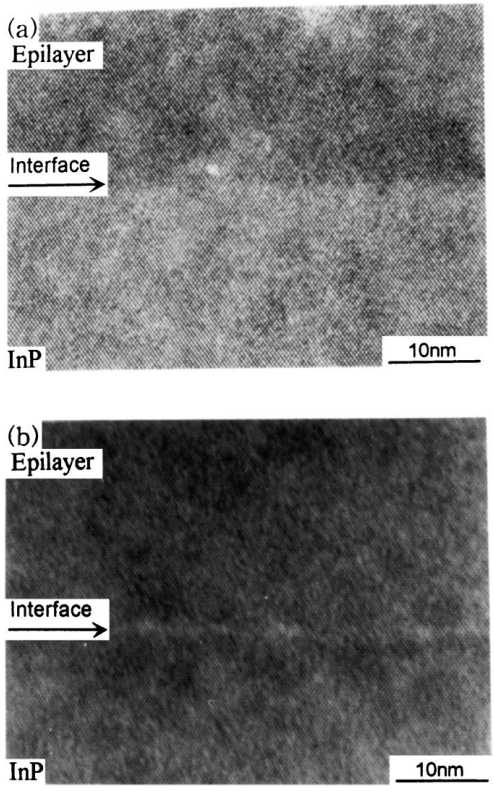

Figure 4 Cross-section HREM images in [110] zone of $In_xAl_{1-x}As$ layers grown on (001) InP; (a) $In_{0.52}Al_{0.48}As$ and (b) $In_{0.489}Al_{0.511}As$.

to be about tens of nanometers. We also observed the modulation contrasts aligned along the [100] and [010] directions in the two-beam images of Figs 2 and 3. But the modulation contrasts are rather faint as compared with those in InGaAs layers. The interval of the modulation contrast is measured to be about 8 nm. This value is nearly same as what can be deduced from the optical and transport investigation properties by Hong *et al.* [9].

Fig. 4 shows cross-section HREM images in [110] zone respectively of $In_{0.52}Al_{0.48}As$ and $In_{0.489}Al_{0.511}As$. The interfaces with the substrate InP are cleanly visible. The $In_{0.52}Al_{0.48}As$ layer shows a relatively flat but contrasted interface with InP substrate. But the interface of the $In_{0.489}Al_{0.511}As$ layer is corrugated. It is note-worthy that the interface divides brightly contrasted substrate regions different both from the darker epilayers. The brightly contrast region is located slightly inside the $In_{0.52}Al_{0.48}As$ layer but it is located at the interface of the $In_{0.489}Al_{0.511}As$ layer and the substrate.

It was previously reported that the brightly contrast regions are in fact inhomogeneities which were composed of InAs or $InAs_yP_{1-y}$ formed by an exchange P with As atoms during preheating to remove the native oxide on InP substrate [20, 21]. These inhomogeneities have been known to influence the structural quality of InAlAs layer and to be the origin of defects such as staking faults, dislocation and clusters [22, 23]. But, in the particular specimen defects associated with these inhomogeneities were not observed.

The interface regions of $In_{0.52}Al_{0.48}As$ and $In_{0.489}Al_{0.511}As$ layers which contain again bright contrast regions are shown in higher magnification in Fig. 5. As expected, the $In_{0.52}Al_{0.48}As$ layer with the In composition of better misfit shows an excellent matching between the substrate and the epilayer. Moreover, the $In_{0.489}Al_{0.511}As$ layer having the lattice misfit of 0.24% with the 1.156 μm thick InP substrate reveals a good lattice matching too. In Fig. 6, the photoluminescence spectra obtained at 77 K from $In_{0.52}Al_{0.48}As$ and $In_{0.489}Al_{0.511}As$ layers are plotted. The spectra consist of two peaks each from the InP substrate and the InAlAs layer. The main exciton

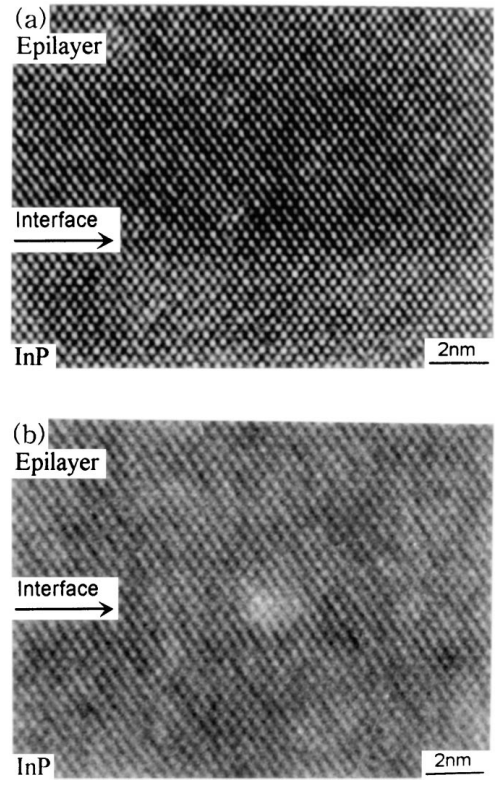

Figure 5 [110] HREM images of $In_{0.52}Al_{0.48}As$ and $In_{0.489}Al_{0.511}As$ layers.

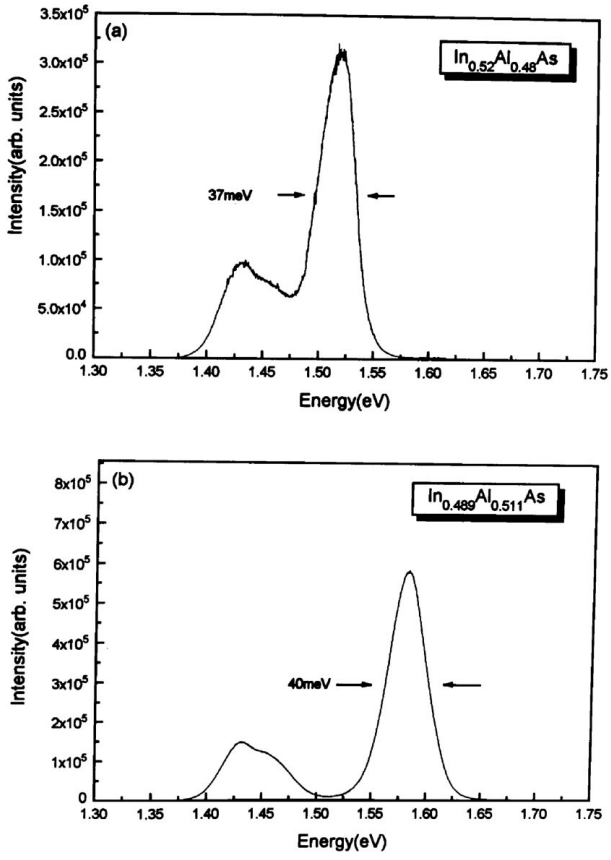

Figure 6 Photoluminescence emission spectra of the $In_xAl_{1-x}As$ layer at 77 K; (a) $In_{0.52}Al_{0.48}As$ and (b) $In_{0.489}Al_{0.511}As$.

transitions of $In_{0.52}Al_{0.48}As$ and $In_{0.489}Al_{0.511}As$ layer are centered at 1.517 and 1.582 eV respectively and their FWHM are 37 and 40 meV. In these spectra, a broad line of the InP substrate appears around 1.431 eV. The intense and narrow bond exciton emission indicates the excellent quality of our specimens grown at 520°C.

The InAlAs layers with a high crystalline quality on InP are reportedly difficult to grow at 500–520°C [4–6, 8, 15]. Our DCXD and our narrow width PL results otherwise show that the $In_{0.52}Al_{0.48}As$ and $In_{0.489}Al_{0.511}As$ layers grown on InP substrates at 520°C reveal an excellent crystalline quality and a good optical performance. This improvement of the crystalline quality of InAlAs layers is derived from the fact that our specimens are relatively free of defects especially at the interfaces. Our conventional TEM and HREM observations have partially supported the above evidences.

Although the $In_{0.489}Al_{0.511}As$ layer has a lattice mismatch of 0.23% and a thickness of 1.156 μm, which is eighteen times larger than the critical thickness of Mattews and Blakeslee [24], it shows the PL characteristics of very high crystalline quality and an excellent lattice matching between the InP substrate and the epilayer. As discussed in the contrast images of the $In_{0.489}Al_{0.511}As$ layer, Figs 4 and 5, compositional inhomogeneities at the interface between the substrate and the epilayer which most likely occur during native oxide desorption of the substrate are present. We infer that the inhomogeneities actually act as a buffer layer accommodating the strain associated with the lattice mismatch. There is a supporting report that the buffer layer improves the epilayer crystalline quality [15]. Hence, the high crystalline quality of $In_{0.489}Al_{0.511}As$ layer may be explained by the existence of buffering inhomogeneities.

Up to now, it was widely known that clustering deteriorates the crystalline quality of epilayers [14, 15]. In the microstructural observations of $In_{0.52}Al_{0.48}As$ and $In_{0.489}Al_{0.511}As$ layers, we observed the lattice modulations most likely accrued to clustering about 8 nm in size. But, in spite of the existence of lattice modulation, the MBE grown $In_{0.52}Al_{0.48}As$ and $In_{0.489}Al_{0.511}As$ layers show crystalline coherency with the substrate. Yet further studies are necessary to understand the exact relation between crystalline quality and clustering in the InAlAs layer.

3.2. Relaxation of the lattice mismatch in $In_{0.476}Al_{0.524}As$ epilayer

The lattice mismatch between substrate and epilayer in most III-V heteroepitaxial systems is reportedly relieved by misfit dislocations [25]. At the same time, there are other reports [26, 27] that stacking faults are responsible for misfit strain relief at the interface of the InGaAs on InP. But the relaxation of lattice mismatch has rarely been reported in InAlAs on InP. Thus we have chosen $In_{0.476}Al_{0.524}As$ which has the relatively high lattice 0.32% mismatch with the InP substrate to study the defect microstructure.

Fig. 7 shows the microstructure of an $In_{0.476}Al_{0.524}As(t = 1.14\ \mu m)$ layer grown at 520°C. In

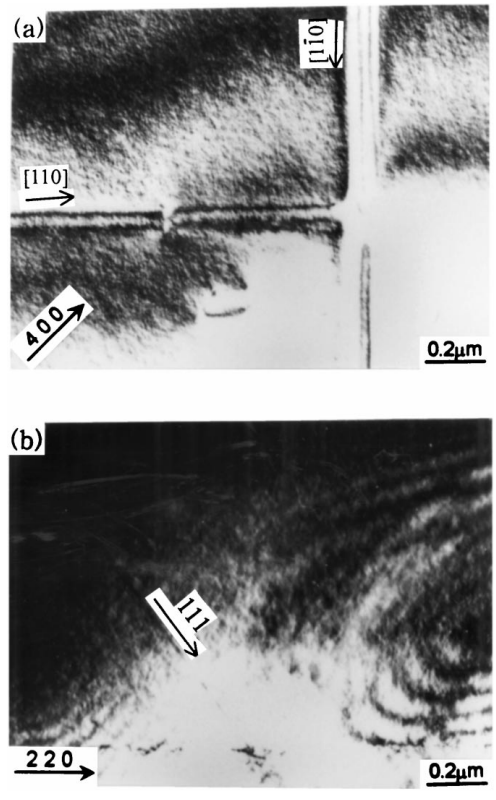

Figure 7 Microstructures of a $In_{0.476}Al_{0.524}As$ layer showing the stacking faults; (a) BF image of $\boldsymbol{g} = 040$ in TEM planar view and (b) BF image of $\boldsymbol{g} = 004$ in the TEM cross-sectional view.

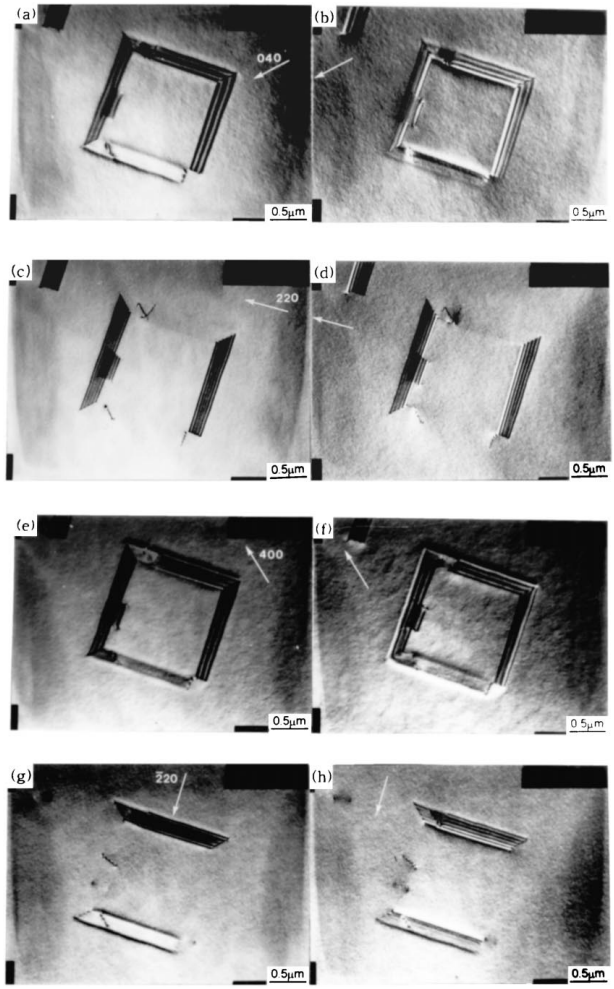

Figure 8 TEM planar view images of a $In_{0.476}Al_{0.524}As$ layer showing a square stacking fault; (a) and (b) are BF and DF images of $\boldsymbol{g} = 040$, respectively, (c) and (d) are BF and DF images of $\boldsymbol{g} = 220$, respectively, (e) and (f) are BF and DF images of $\boldsymbol{g} = 400$, respectively, (g) and (h) are BF and DF images of $\boldsymbol{g} = 220$, respectively.

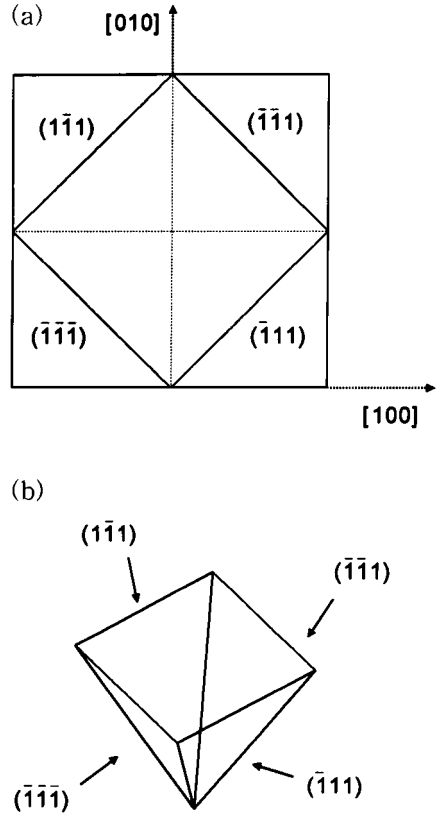

Figure 9 A schematic showing the pyramidal stacking fault plane.

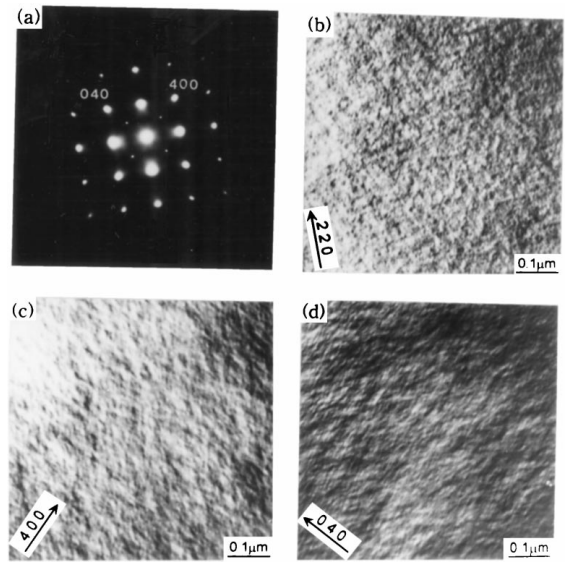

Figure 10 TEM planar view of the $In_{0.476}Al_{0.524}As$ layer; (a) [001] zone diffraction pattern, (b), (c) and (d) are a series of DF images obtained from the specimens in (220), (400) and (040) two beam conditions, respectively.

contrast to the already mentioned microstructures of $In_{0.52}Al_{0.48}As$ and $In_{0.489}Al_{0.511}As$ layers, stacking faults parallel to the two mutually orthogonal [110] and [$\bar{1}$10] directions are revealed in Fig. 7a. Also, a stacking fault extended from the interface to the free surface is present in the cross-sectional view of Fig. 7b.

In addition to the stacking faults parallel to the [110] and [$\bar{1}$10] directions, square type stacking faults are also observed in the $In_{0.476}Al_{0.524}As$ layer, but their occurrence is rare. In order to understand three dimensional character of these faults, a series of tilting experiments of a TEM specimen has been carried out. The bright and dark field images obtained from various two beam conditions are shown in Fig. 8. The stacking fault planes were determined by the extinction of their contrast at each operating $\boldsymbol{g}$ vector and the nature of stacking fault was analyzed by the variation of its contrast in bright and dark field when the same $\boldsymbol{g}$ operates [28]. From the extinction behavior both of bright and dark field fault images and brightness image contrast as described in the reference [28], we can determine the stacking fault characteristics. A schematic showing the three dimensional structure derived from the analyzed results can be constructed as in Fig. 9. We see that the square type stacking fault in planar view is pyramidal type in three dimension.

Stacking faults of the type as shown in Fig. 7 are more common and are distributed throughout the epilayers. Other types of defects, especially, dislocations are hardly observed. These results indicate that the lattice mismatch of $In_{0.476}Al_{0.524}As$ layer is relaxed by the formation of stacking faults. Also, because $In_{0.489}Al_{0.511}As$ and $In_{0.476}Al_{0.524}As$ layers have nearly the same thickness, we deduce from the microstructural

results that the relaxation of the lattice mismatch between the substrate and the epilayer start at a certain In composition between 0.489 and 0.476.

Fig. 10 shows the microstructure of a region between stacking faults inside the $In_{0.476}Al_{0.524}As$ layer. It reveals the modulation contrast aligned along the [100] and [010] direction respectively and indicates the occurrence of clustering in the $In_{0.476}Al_{0.524}As$ layer too. The separation of the modulation contrasts are measured to be about 8 nm. From the microstructural studies, it is found that clustering occurs in the $In_{0.476}Al_{0.524}As$ layer is similar to the mode in the $In_{0.52}Al_{0.48}As$ and $In_{0.489}Al_{0.511}As$ layers. In regards to InGaAs layer, there are some reports [19, 29] that the wavelength of modulation contrast is dependent upon the lattice mismatch between the substrate and the epilayer. But our results indicate that the size of clusters is about 8 nm irrespective of the lattice mismatch in the $In_xAl_{1-x}As$ ($x = 0.52$, 0.489, 0.476) thin films.

4. Conclusion

We have studied the crystalline quality and optical properties of $In_xAl_{1-x}As$ layers ($x = 0.52$, 0.489) and the misfit strain relief in $In_{0.476}Al_{0.524}Al$ layer grown at 520°C by MBE on InP substrates. We observed the growth of not only $In_{0.52}Al_{0.48}As$ but also $In_{0.489}Al_{0.511}As$ layers with both high structural quality and optical performance under our growth conditions. Especially, in the $In_{0.489}Al_{0.511}As$ layer, the observed linewidth of the double crystal x-ray diffraction peak is practically same as that of the theoretically calculated on of the perfect crystal.

TEM and HREM images of $In_{0.52}Al_{0.48}As$ and $In_{0.489}Al_{0.511}As$ layers show clean crystal structures and excellent lattice matching between the substrate and the epilayer. In case of the $In_{0.489}Al_{0.511}As$ layer having the lattice mismatch of 0.23%, it is deduced that perfect lattice matching is achieved by the accommodation of stain associated with the lattice mismatch by inhomogeneities formed during the oxide desorption.

From TEM observations, we find that the lattice mismatch of the $In_{0.476}Al_{0.524}As$ layer is relaxed by the formation of the stacking faults. The pyramidal stacking faults are observed but only rarely in the $In_{0.476}Al_{0.52}As$ layer.

Acknowledgement

This study was supported by the academic research fund of Ministry of Education, Republic of Korea, through Inter-University Semiconductor Research Center (ISRC 97-E-0000) in Seoul National University.

References

1. J. P. PRASEUTH, L. GOLDSTEIN, P. HENOC, J. PRIMOT and G. DANAN, *J. Appl. Phys.* **61** (1987) 215.
2. P. R. BERGEN, P. K. BHATTACHARYA and J. SINGH, *ibid.* **61** (1987) 2856.
3. F. Y. JUNAG, W. P. HONG, P. R. BERGER, P. K. BHATACHARYA, U. DAS and J. SINGH, *J. Cryst. Growth* **81** (1987) 373.
4. B. GOLDSTEIN and D. SZOSTAK, *Appl. Phys. Lett.* **26** (1975) 685.
5. C. T. FOXON and B. A. JOYCE, *J. Cryst. Growth* **44** (1978) 75.
6. C. E. C. WOOD, D. V. MORGAN and L. RATHBUN, *J. Appl. Phys.* **53** (1982) 4524.
7. K. NAJAAJIMA, T. TANAHASHI and K. AKITA, *Appl. Phys. Lett.* **41** (1982) 194.
8. J. SINGH, S. BUDLEY, B. DAVIES and K. K. BAJAJ, *J. Appl. Phys.* **60** (1987) 3167.
9. W. P. HONG, P. K. BHATTACHARYA and J. SINGH, *Appl. Phys. Lett.* **50** (1987) 618.
10. P. CHU, C. LIN and H. H. WIEDER, *ibid.* **53** (1988) 2423.
11. J. H. MARSH, *ibid.* **4** (1982) 732.
12. N. HOLONYAK, W. D. LAIDIG, M. D. CAMRAS, H. MORKOC, T. J. DRUMMOND, K. HESS and M. S. BURROUGHS, *J. Appl. Phys.* **52** (1981).
13. J. E. OH, P. K. BHATTACHARYA, Y. C. CHEN, O. AINA and M. MATTINGLY, *J. Electron Mater.* **19** (1990) 435.
14. D. F. WELCH, G. W. WICKS, L. F. EASTMAN, P. PARAYANTAL and F. H. POLLAK, *Appl. Phys. Lett.* **46** (1985) 169.
15. E. TOURNIE, Y.-H. ZHANG, N. J. PULSFORD and K. PLOOG, *J. Appl. Phys.* **70** (1991) 7362.
16. B. R. BENETT and J. A. DEL ALAMO, *ibid.* **73** (1993) 3195.
17. S. N. G. CHU, S. NAKAHARA, K. E. STREGE and W. D. JOHNSTON, JR., *ibid.* **57** (1985) 4610.
18. T. L. MCDEVITT, S. MAHAJAN, D. E. LAUGHLIN, W. A. BONNER and V. G. KERAMIDAS, *Phys. Rev.* **B45** (1992) 6614.
19. F. PEIRO, A. CORNET, A. HERMS, J. R. MORANTE, S. A. CLARK and R. H. WILLIAMS, *J. Appl. Phys.* **73** (1993) 4319.
20. J. M. MOISON, M. BENSOUSSAN and F. HOUZAY, *Phys. Rev.* **B33** (1986) 2018.
21. J. M. VANDENBERG, A. T. MACRANDER, R. A. HAMM and M. B. PANISH, *ibid.* **B44** (1991) 3391.
22. E. CARLINO, C. GIANNIN, L. TAPFER, M. CATALANO, E. TOURNIE, Y. H. ZHANG, K. H. PLOOG, *J. Appl. Phys.* **78** (1995) 2403.
23. F. PEIRO, A. CORNET, A. HERMS, J. R. MORANTE, A. GEORGAKILAS and G. HALKIAS, *J. Vac. Sci. Technol.* **B10** (1992) 2148.
24. J. W. MATTHEWS and A. E. BLAKESLEE, *J. Cryst. Growth* **27** (1974) 118.
25. J. W. MATTHEWS in "Epitaxial Growth, Part B," edited by J. W. Matthews (Academic, New York, 1975) pp. 560–610.
26. S. N. G. CHU, A. T. MACRANDER, K. E. STREGE and W. D. JOHNSTON, JR., *J. Appl. Phys.* **57** (1985) 249.
27. N. G. CHEW, A. G. CULLIS, S. J. BASS, L. L. TAYLOR, M. S. SKOLNICK and A. D. PITT, Inst. Phys. Conf. Ser. No. 87 (1987).
28. P. B. HIRSCH, A. HOWIE, R. B. NICHOLSON, D. W. PASHLEY and M. J. WHELAN, "Electron Microscopy of Thin Crystal" (E.K. Robert, New York, 1977) p. 229.
29. P. LETARDI, N. MOTTA and A. BALZAROTTI, *Solid State Phys.* **20** (1987) 2853.
30. A. S. BROWN, M. J. DALANCY and J. SINGH, *J. Vac. Sci. Technol.* **B7** (1989) 384.

Received 21 August 1998
and accepted 22 July 1999